

# Trade-offs between retroactivity and noise in connected transcriptional components

Narmada Herath<sup>1</sup> and Domitilla Del Vecchio<sup>2</sup>

**Abstract**—At the interconnection of two gene transcriptional components in a biomolecular network, the noise in the downstream component can be reduced by increasing its gene copy number. However, this method of reducing noise increases the load applied to the upstream system, called retroactivity, thereby causing a perturbation in the upstream system. In this work, we quantify the error in the system trajectories caused by perturbations due to retroactivity and noise, and analyze the trade-off between these two perturbations. We model the system as a set of nonlinear chemical Langevin equations and quantify the trade-off by employing contraction theory for stochastic systems.

## I. INTRODUCTION

The notion of modularity within networks has been recognized as a key feature linking biology to engineering [1], [2]. In particular, many studies in systems biology have focused on identifying functional modules in biological networks [3], [4]. Modularity also plays a fundamental role in the emerging field of synthetic biology, where the goal is to build biological units that can be interconnected to form networks performing different tasks [5].

However, a problem that has been identified is the inability of modules to maintain their pre-characterized behavior upon interconnection. This is due to loading effects between modules that appear at interconnections, similar to loading effects in electrical circuits. This effect is termed ‘retroactivity’ [4], [6], and is known to increase with increasing downstream load [6]. Retroactivity is also linked to the notion of ‘fan-out’, which is defined as the maximum number of downstream components that can be regulated by an upstream transcriptional factor, without altering the dynamics of the output of the upstream component [7]. The impact of retroactivity has been verified experimentally in gene transcriptional modules [8] and in signal transduction networks [9].

A characteristic of biological networks is the stochasticity due to intrinsic and extrinsic noise. Intrinsic noise is inherently present in the cell due to randomness in chemical reactions and low copy numbers of molecules [10], [11], [12], [13]. Extrinsic noise is caused by variations in the cellular environment such as the number of metabolites, ribosomes and polymerases [10], [11], [12]. As intrinsic noise is inevitable, the study of its effects is important in understanding cellular behavior and designing new biological

networks. In general, the noise in a species is assessed using the coefficient of variation, defined as the ratio between the standard deviation and the mean of the species concentration [11], [12], [14]. Theoretically, it has been predicted that the intrinsic noise of a species, quantified this way, is inversely proportional to the square root of the number of molecules of the species [14], [15], [16]. This relation has been studied extensively in gene expression [11], [12], [13], [10], [14]. In particular, Swain et al. [12] have shown that increasing the gene copy number decreases the intrinsic noise in the protein being expressed. Studies also suggest that exact gene duplication and redundancy may also function as natural mechanisms by which a cell attenuates stochastic effects in gene expression [14], [17]. Therefore the control of gene copy number is a method of reducing protein noise in gene expression [14].

However, in a biological network, increasing the gene copy number of a downstream component increases the retroactivity to the upstream system. Therefore, it is necessary to seek a compromise between attenuating noise and increasing retroactivity in the network. There have been previous studies that consider the compromise between retroactivity and noise, but these studies focus on the noise in the output of the upstream component [18], [19]. Hence, the trade-off between suppressing noise in the downstream system and increasing retroactivity to the upstream system has not yet been quantified.

In this work, we consider an interconnection of two transcriptional components and quantify the above trade-off for different system models. Similar to the coefficient of variation, we use the ratio of signal error to its nominal value to quantify the effect of each of the perturbations. The stochastic nature of the system is modeled using the chemical Langevin equation. We first consider the system linearized about a fixed point and then analyze the nonlinear system using stochastic contraction theory [20] to provide an upper bound for the error due to noise. Our analytical results show that increasing the gene copy number minimizes the upper bound for the error due to noise but this leads to an increase in the magnitude of the error due to retroactivity.

This paper is organized as follows. In Section II, the system studied is introduced and the mathematical model is derived using the chemical Langevin equation. Section III quantifies the trade-off for the system linearized about a fixed point. In Section IV, an extension to the stochastic contraction theory is introduced and the trade-off is analyzed for the nonlinear model.

<sup>1</sup>Narmada Herath is with the Department of Electrical Engineering and Computer Science, Massachusetts Institute of Technology, 77 Mass. Ave, Cambridge MA nherath@mit.edu

<sup>2</sup>Domitilla Del Vecchio is with the Department of Mechanical Engineering, Massachusetts Institute of Technology, 77 Mass. Ave, Cambridge MA ddv@mit.edu

## II. SYSTEM MODEL AND PROBLEM FORMULATION

A typical instance of an interconnection between two transcriptional components is what found in a reporter system (Fig. 1). In order to measure the concentration of protein Y, we use a downstream component, which acts as a measuring device, producing the reporter protein G that has easily measurable characteristics, such as fluorescence. Protein Y acts as an activator to the downstream component, therefore, the concentration of protein G is proportional to that of Y. As a result, the concentration of protein G can be used as an indicator for the concentration of Y. The chemical

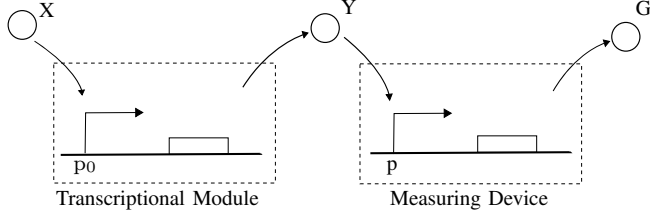


Fig. 1: The upstream transcriptional component takes protein X as the input, and produces the output protein Y. The downstream transcriptional component takes protein Y as the input and produces protein G as the output.

reactions for the upstream component in Fig. 1 are as follows:  $X + p_0 \xrightleftharpoons[\alpha_2]{\alpha_1} C_0$ ,  $C_0 \xrightarrow{\beta_1} Y + C_0$ ,  $Y \xrightarrow{\delta_1} \phi$ . Protein X binds to promoter  $p_0$  and produces the complex  $C_0$  where  $\alpha_1$  and  $\alpha_2$  are the association and dissociation rate constants, respectively.  $\beta_1$  is the total production rate constant of protein Y lumping both transcription and translation together.  $\delta_1$  is the decay rate constant of Y accounting for degradation and dilution. A similar set of reactions can be written for the downstream component:  $Y + p \xrightleftharpoons[\alpha_4]{\alpha_3} C$ ,  $C \xrightarrow{\beta_2} G + C$ ,  $G \xrightarrow{\delta_2} \phi$ .

Let the total concentrations of promoters in the upstream and downstream components be  $p_{t0}$  and  $p_t$ , respectively. Since the total concentration of promoter is conserved, we can write the conservation laws  $p_{t0} = p_0 + C_0$  and  $p_t = p + C$ . Let  $\Gamma_i$  for  $i = 1, \dots, 8$  be independent Gaussian white noise processes and  $\Omega$  be the cell volume. Then, the chemical Langevin equations are given by (assuming  $\Omega = 1$  for simplicity)

$$\begin{aligned} \dot{C}_0 &= \alpha_1 X(p_{t0} - C_0) - \alpha_2 C_0 + \sqrt{\alpha_1 X(p_{t0} - C_0)} \Gamma_1 \\ &\quad - \sqrt{\alpha_2 C_0} \Gamma_2, \\ \dot{Y} &= \beta_1 C_0 - \delta_1 Y + \sqrt{\beta_1 C_0} \Gamma_3 - \sqrt{\delta_1 Y} \Gamma_4 \boxed{+ \alpha_4 C} \\ &\quad \boxed{- \alpha_3 Y(p_t - C) - \sqrt{\alpha_3 Y(p_t - C)} \Gamma_5 + \sqrt{\alpha_4 C} \Gamma_6}, \\ \dot{C} &= \alpha_3 Y(p_t - C) - \alpha_4 C + \sqrt{\alpha_3 Y(p_t - C)} \Gamma_5 \\ &\quad - \sqrt{\alpha_4 C} \Gamma_6, \\ \dot{G} &= \beta_2 C - \delta_2 G + \sqrt{\beta_2 C} \Gamma_7 - \sqrt{\delta_2 G} \Gamma_8. \end{aligned} \quad (1)$$

The terms multiplied by  $\Gamma_i$  represent the intrinsic noise in the corresponding reactions and the boxed terms represent

the retroactivity from the downstream component to the upstream system.

Separation of timescales is a common feature in biomolecular systems and we use this property to perform model order reduction for system (1). Binding/unbinding reactions are much faster than protein production/decay, therefore, we can write  $\alpha_2 \gg \delta_1$ . Let  $k_{d1} = \alpha_2/\alpha_1$  and  $k_{d2} = \alpha_4/\alpha_3$  be the dissociation constants. To take the system into standard singular perturbation form [21], write  $\epsilon = \delta_1/\alpha_2$  where  $\epsilon \ll 1$  and let  $a = \alpha_4/\alpha_2$ . Then, with the change of variable  $y = Y + C$ , we can take the system to the standard singular perturbation form

$$\begin{aligned} \epsilon \dot{C}_0 &= (\delta_1/k_{d1})X(p_{t0} - C_0) - \delta_1 C_0 \\ &\quad + \sqrt{(\epsilon\delta_1 k_{d1})X(p_{t0} - C_0)} \Gamma_1 - \sqrt{\epsilon\delta_1 C_0} \Gamma_2, \\ \dot{y} &= \beta_1 C_0 - \delta_1(y - C) + \sqrt{\beta_1 C_0} \Gamma_3 \\ &\quad - \sqrt{\delta_1(y - C)} \Gamma_4, \\ \epsilon \dot{C} &= (a\delta_1/k_{d2})(y - C)(p_t - C) - a\delta_1 C \\ &\quad + \sqrt{(a\epsilon\delta_1 k_{d2})y - C}(p_t - C) \Gamma_5 - \sqrt{a\epsilon\delta_1 C} \Gamma_6, \\ \dot{G} &= \beta_2 C - \delta_2 G + \sqrt{\beta_2 C} \Gamma_7 - \sqrt{\delta_2 G} \Gamma_8 \end{aligned}$$

where  $y$  and  $G$  are the slow variables of the system. By setting  $\epsilon = 0$ , we obtain the reduced order dynamics of Y and G on the slow manifold, which can be shown to be locally exponentially stable. Using that  $\Gamma_i$  are independent identical Gaussian white noise processes, these dynamics are given by

$$\begin{aligned} \dot{Y} &= (1 - R(Y))(\beta_1 p_{t0} X/(X + k_{d1}) - \delta_1 Y \\ &\quad + \sqrt{\beta_1 p_{t0} X/(X + k_{d1}) + \delta_1 Y} \Gamma_Y), \\ \dot{G} &= \beta_2 p_t Y/(Y + k_{d2}) - \delta_2 G \\ &\quad + \sqrt{\beta_2 p_t Y/(Y + k_{d2}) + \delta_2 G} \Gamma_G, \end{aligned}$$

with  $R(Y) = \frac{1}{1 + (Y + k_{d2})^2/(p_t k_{d2})}$ . In this work, we assume that  $X \ll k_{d1}$  and  $Y \ll k_{d2}$ , implying weak binding, resulting in the system :

$$\begin{aligned} \text{System 4: } \dot{Y} &= (1 - R)(\beta_1 p_{t0} X/k_{d1} - \delta_1 Y \\ &\quad + \sqrt{\beta_1 p_{t0} X/k_{d1} + \delta_1 Y} \Gamma_Y), \\ \dot{G} &= \beta_2 p_t Y/k_{d2} - \delta_2 G \\ &\quad + \sqrt{\beta_2 p_t Y/k_{d2} + \delta_2 G} \Gamma_G, \end{aligned} \quad (2)$$

with  $R = \frac{1}{1 + k_{d2}/p_t}$ , where the noise terms are nonlinear factors of the state. We define this system (2) - (3) as the ‘perturbed system’ due to the presence of the perturbations given by the retroactivity and noise. This system is illustrated in System 4 in Fig. 3. We also define a ‘nominal system’ (System 1 in Fig. 3) that gives the ideal system behavior in the absence of these perturbations:

$$\text{System 1: } \dot{Y}_N = \beta_1 p_{t0} X/k_{d1} - \delta_1 Y_N, \quad (4)$$

$$\dot{G}_N = \beta_2 p_t Y_N/k_{d2} - \delta_2 G_N. \quad (5)$$

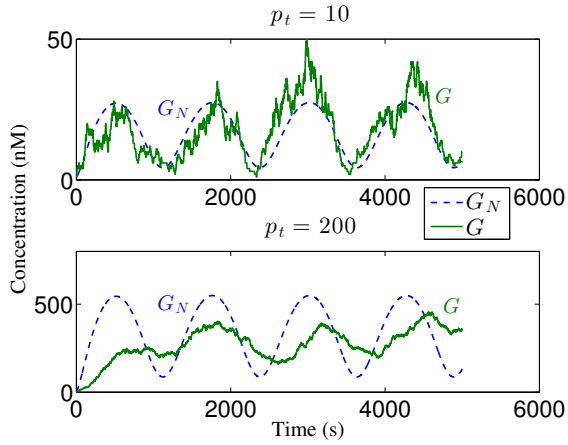


Fig. 2: Nominal and perturbed signals.  $G$  is obtained by simulating system (1) using the Gillespie algorithm [22]. The parameter values are  $X = 1 + \sin(\omega t)$  nM,  $\alpha_1 = 1$  nMs $^{-1}$ ,  $\alpha_2 = 10$  s $^{-1}$ ,  $\alpha_3 = 1$  nMs $^{-1}$ ,  $\alpha_4 = 20$  s $^{-1}$ ,  $\beta_1 = 0.01$  s $^{-1}$ ,  $\beta_2 = 0.1$  s $^{-1}$ ,  $\delta_1 = \delta_2 = 0.01$  s $^{-1}$ ,  $p_{t0} = 50$  nM and  $\omega = 0.005$  rad/s.

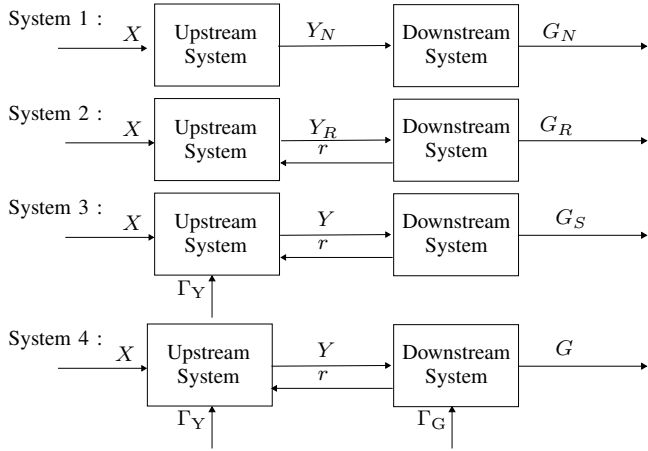


Fig. 3: Retroactivity to the upstream is denoted by ‘r’. System 1 represents the flow of nominal signals in the absence of any perturbations. System 2 represents the flow of signals when the system is perturbed only with retroactivity. System 3 represents the flow of signals when the system is perturbed with retroactivity and noise in the upstream component. System 4 represents the flow of signals when the system perturbed with retroactivity and intrinsic noise in both components.

Fig. 2 illustrates the nominal and perturbed trajectories of  $G$  for different copy numbers of downstream components ( $p_t$ ). It can be seen that for low amounts of downstream components, the perturbed signal closely tracks in average the nominal signal but the perturbation due to noise is high. For high amounts of downstream components there is less noise but the tracking is lost due to retroactivity. Therefore, we can see that there is a trade-off between attenuating noise and maintaining signal accuracy as the value of  $p_t$  is increased. In this work, we quantify this trade-off mathematically. To this end, we define each of the perturbations by introducing the errors  $\Delta G_R = G_R - G_N$  and  $\Delta G_P = G - G_R$ , which represent the perturbations due to retroactivity and noise,

respectively (Fig. 3). We denote by  $G_e$  the steady state value of  $G_N$ , and quantify the retroactivity through  $\frac{|\Delta G_R|}{G_e}$ . The error due to noise is quantified by finding a function  $A(p_t)$  such that  $\frac{\sqrt{E[|\Delta G_P|^2]}}{G_e} \leq A(p_t)$ .

To quantify the errors due to retroactivity and noise we use the following intermediate systems (see Fig. 3). System 2 represents the upstream and downstream dynamics when the components are perturbed only with retroactivity. The reduced dynamics for this system are given by

$$\text{System 2 : } \dot{Y}_R = (1 - R)(\beta_1 p_{t0} X / k_{d1} - \delta_1 Y_R), \quad (6)$$

$$\dot{G}_R = \beta_2 p_t Y_R / k_{d2} - \delta_2 G_R. \quad (7)$$

In System 3, the upstream component is perturbed with noise  $\Gamma_Y$ , in addition to retroactivity. The reduced dynamics of this system are given by

$$\text{System 3 : } \dot{Y} = (1 - R)(\beta_1 p_{t0} X / k_{d1} - \delta_1 Y) \quad (8)$$

$$+ \sqrt{\beta_1 p_{t0} X / k_{d1} + \delta_1 Y} \Gamma_Y,$$

$$\dot{G}_S = \beta_2 p_t Y / k_{d2} - \delta_2 G_S. \quad (9)$$

We assume that solutions exist and that they are unique for the above system equations.

### III. LINEARIZED ANALYSIS

In this section, as an initial step in analyzing the trade-off, we consider the system linearized about the steady state, assuming small amplitude signals.

Given the constant inputs  $X_e, \Gamma_Y = \Gamma_G = 0$  and the corresponding steady state  $Y_e = (\beta_1 X_e p_{t0}) / (\delta_1 k_{d1})$ , and  $G_e = (\beta_2 Y_e p_t) / (\delta_2 k_{d2})$ , we consider the linearization of system (2) - (3) about this steady state. To this end, let  $\tilde{X} = X - X_e$ ,  $\tilde{Y} = Y - Y_e$ ,  $\tilde{G} = G - G_e$ ,  $\tilde{\Gamma}_Y = \Gamma_Y$ , and  $\tilde{\Gamma}_G = \Gamma_G$ . Then the linearized perturbed system (System 4) is given by

$$\dot{\tilde{Y}} = (1 - R)(\beta_1 p_{t0} \tilde{X} / k_{d1} - \delta_1 \tilde{Y}) \quad (10)$$

$$+ \sqrt{2\beta_1 p_{t0} X_e / k_{d1}} \tilde{\Gamma}_Y,$$

$$\dot{\tilde{G}} = \beta_2 p_t \tilde{Y} / k_{d2} - \delta_2 \tilde{G} + \sqrt{2\beta_2 p_t Y_e / k_{d2}} \tilde{\Gamma}_G.$$

To find the error due to retroactivity, consider System 1 and System 2 in Fig. 3, for which the dynamics are given by (4) - (5) and (6) - (7). We denote by  $\Delta Y_R = Y_R - Y_N$ , the error in the upstream output when the system is perturbed with only retroactivity. Let  $\tilde{Y}_N = Y_N - Y_e$ ,  $\tilde{G}_N = G_N - G_e$ ,  $\tilde{Y}_R = Y_R - Y_e$ , and  $\tilde{G}_R = G_R - G_e$ , be the perturbations about the steady state for the two systems. Thus, we can write  $\Delta \tilde{Y}_R = \tilde{Y}_R - \tilde{Y}_N$  and  $\Delta \tilde{G}_R = \tilde{G}_R - \tilde{G}_N$ . Since systems (4) - (5) and (6) - (7) are linear we can evaluate directly their frequency response.

Considering a periodic input of the form  $\tilde{X} = k_2 \sin(\omega t)$  and using that  $R = \frac{1}{1 + k_{d2}/p_t}$ , we obtain

$$\frac{|\Delta \tilde{G}_R(j\omega)|}{G_e} = \frac{p_t \omega \delta_1 \delta_2 |k_2|}{X_e \sqrt{(\omega^2 + \delta_2^2)(\omega^2 + \delta_1^2)(\omega^2(p_t + k_{d2})^2 + k_{d2}^2 \delta_1^2)}}. \quad (11)$$

Therefore the error due to retroactivity increases as  $p_t$  increases.

To determine the error due to noise we consider System 4 and System 2 (Fig. 3) that has the dynamics (2) - (3) and (6) - (7), respectively. We denote by  $\Delta Y_S = Y - Y_R$ , the error in the output of the upstream component, caused by noise  $\Gamma_Y$ . Considering the linearized system (10) we can write  $\Delta \dot{Y}_S = \dot{Y} - \dot{Y}_R$  and  $\Delta \dot{G}_P = \dot{G} - \dot{G}_R$ . Then, using (6) - (7) and (10) we obtain

$$\begin{aligned}\Delta \dot{Y}_S &= (1 - R)(\sqrt{2\beta_1 p_{t0} X_e / k_{d1}} \Gamma_Y - \delta_1 \Delta \tilde{Y}_S), \quad (12) \\ \Delta \dot{G}_P &= \beta_2 p_t \Delta \tilde{Y}_S / k_{d2} - \delta_2 \Delta \tilde{G}_P + \sqrt{2\beta_2 p_t Y_e / k_{d2}} \Gamma_G.\end{aligned}\quad (13)$$

Let the power spectral densities of  $\Delta \tilde{Y}_S$  and  $\Gamma_G$  be  $S_{\Delta \tilde{Y}_S}(j\omega)$  and  $S_{\Gamma_G}(j\omega)$ , respectively. Since  $\Delta \tilde{Y}_S$  and  $\Gamma_G$  are independent, zero mean Gaussian processes, we obtain that their cross-correlation is zero. Then, since they are stationary processes, we determine the power spectral density of  $\Delta \tilde{G}_P$  [23] to be

$$\begin{aligned}S_{\Delta \tilde{G}_P}(j\omega) &= \frac{(\beta_2 p_t / k_{d2})^2}{\omega^2 + \delta_2^2} S_{\Delta \tilde{Y}_S}(j\omega) \\ &\quad + \frac{2\beta_2 p_t Y_e / k_{d2}}{\omega^2 + \delta_2^2} S_{\Gamma_G}(j\omega).\end{aligned}\quad (14)$$

Since  $\Gamma_G$  is a Gaussian white noise process,  $S_{\Gamma_G}(j\omega) = 1$ . The power spectral density of  $\Delta \tilde{Y}_S$  can be determined using (12), where  $\Gamma_Y$  is a Gaussian white noise process with a power spectral density of 1. We find that

$$S_{\Delta \tilde{Y}_S}(j\omega) = \frac{2(1 - R)^2 \beta_1 p_{t0} X_e / (k_{d1})}{\omega^2 + (1 - R)^2 \delta_1^2}.\quad (15)$$

Using (14) and (15), we obtain  $S_{\Delta \tilde{G}_P}(j\omega) = \frac{(\beta_2 p_t / k_{d2})^2}{\omega^2 + \delta_2^2} \frac{2(1 - R)^2 \beta_1 p_{t0} X_e / (k_{d1})}{\omega^2 + (1 - R)^2 \delta_1^2} + \frac{2\beta_2 p_t Y_e / k_{d2}}{\omega^2 + \delta_2^2}$ . Taking the inverse Fourier transform of  $S_{\Delta \tilde{G}_P}(j\omega)$  gives the autocorrelation  $R_{\Delta \tilde{G}_P}(\tau)$  of  $\Delta \tilde{G}_P$ . Since  $E[|\Delta \tilde{G}_P|^2] = R_{\Delta \tilde{G}_P}(0)$ , we obtain that

$$\begin{aligned}&\sqrt{E[|\Delta \tilde{G}_P|^2]} \\ &\quad \frac{G_e}{\sqrt{\frac{k_{d2} k_{d1} \delta_1 \delta_2}{X_e \beta_1 p_{t0} (\delta_1 k_{d2} + (p_t + k_{d2}) \delta_2)} + \frac{k_{d1} k_{d2} \delta_1 \delta_2}{\beta_2 p_t \beta_1 p_{t0} X_e}}}}.\end{aligned}\quad (16)$$

Therefore, the error due to noise decreases with increasing  $p_t$ . Fig. 4 shows a plot of  $\frac{|\Delta \tilde{G}_P|}{G_e}$  from (11) vs.  $\frac{\sqrt{E[|\Delta \tilde{G}_P|^2]}}{G_e}$  from (16). It can be seen that the two errors vary inversely to each other. Therefore minimizing one of the errors would result in an increase in the other. This illustrates the trade-off between the two perturbations.

#### IV. NONLINEAR ANALYSIS

In this section, we mathematically characterize the trade-off using directly the nonlinear system model (2) - (3). First we introduce the required mathematical tools.

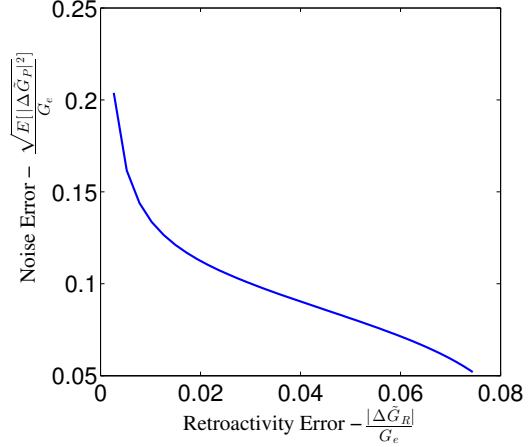


Fig. 4: Trade-off between retroactivity and noise. The parameter values are  $X = 5 + 0.5 \sin(\omega t) \text{ nM}$ ,  $X_e = 5 \text{ nM}$ ,  $\beta_1 = 0.01 \text{ s}^{-1}$ ,  $\beta_2 = 0.1 \text{ s}^{-1}$ ,  $\delta_1 = 0.015$ ,  $\delta_2 = 0.01 \text{ s}^{-1}$ ,  $p_{t0} = 100 \text{ nM}$ ,  $k_{d1} = 10 \text{ nM}$ ,  $k_{d2} = 10 \text{ nM}$  and  $\omega = 0.005 \text{ rad/s}$ .

#### A. Mathematical Tools

**Theorem 1.** (Stochastic Contraction - Extension Theorem 2 in [20].) Consider the following system described by the Itô differential equations

$$\begin{aligned}dx &= \begin{pmatrix} f(a, t) \\ f(b, t) \end{pmatrix} dt + \begin{pmatrix} \sigma(a, t) & 0 \\ 0 & \sigma(b, t) \end{pmatrix} \begin{pmatrix} dW_1^d \\ dW_2^d \end{pmatrix}, \\ &= \hat{f}(x, t) dt + \hat{\sigma}(x, t) dW^{2d},\end{aligned}$$

where  $f$  is a  $\mathbb{R}^n \times \mathbb{R}^+ \rightarrow \mathbb{R}^n$  function,  $\sigma$  is a  $\mathbb{R}^n \times \mathbb{R}^+ \rightarrow \mathbb{R}^{n \times d}$  matrix valued function and  $W_i^d$  are standard  $d$ -dimensional Wiener processes. Assume the system satisfies the following hypotheses:

(H1) There exists a state-independent, uniformly positive definite metric  $M(t) = \Theta(t)^T \Theta(t)$  such that with  $\beta > 0$ ,  $x^T M(t) x \geq \beta \|x\|^2 \forall x, t$ , and  $f$  is contracting [24] in this metric, with contraction rate  $\lambda > 0$ , that is,

$$\lambda_{max} \left( \left( \frac{d}{dt} \Theta(t) + \Theta(t) \frac{\partial f}{\partial a} \right) \Theta^{-1}(t) \right) \leq -\lambda, \forall t, a,$$

where  $\lambda_{max}(Q)$  is the maximum eigenvalue of symmetric part of  $Q$ .

(H2)  $E[\text{tr}(\sigma(a, t)^T M(t) \sigma(a, t))]$  is uniformly upper bounded by a constant  $C$ .

Let  $a(t)$  and  $b(t)$  be two trajectories whose initial conditions are independent of noise and given by a probability distribution  $p(\xi_1, \xi_2)$ . Then,  $\forall t \geq 0$ ,

$$\begin{aligned}E[|a(t) - b(t)|^2] &\leq \frac{1}{\beta} \left( \frac{C}{\lambda} + E[(\xi_1 - \xi_2)^T M(0) (\xi_1 - \xi_2)] e^{-(2\lambda t)} \right).\end{aligned}\quad (17)$$

*Proof.* See Appendix A-2.  $\square$

Theorem 2 in [20] requires  $\text{tr}(\sigma(a, t)^T M(t) \sigma(a, t)) \leq C$  uniformly and globally, in place of (H2). This extension allows us to apply this theorem to systems where  $\sigma(a, t)$  is not uniformly upper bounded for all  $a, t \geq 0$ .

**Corollary 1.** Consider the following augmented system

$$dx = \begin{pmatrix} f(a, t) \\ f(b, t) \end{pmatrix} dt + \begin{pmatrix} 0 & 0 \\ 0 & \sigma(b, t) \end{pmatrix} \begin{pmatrix} dW_1 \\ dW_2 \end{pmatrix}, \quad (18)$$

where  $f(a, t) = -Aa(t) + Bu(t)$  is a  $\mathbb{R} \times \mathbb{R}^+ \rightarrow \mathbb{R}$  function,  $\sigma(b, t) = \sqrt{Ab(t) + Bu(t)}$  is a  $\mathbb{R} \times \mathbb{R}^+ \rightarrow \mathbb{R}$  function with  $A > 0$  and  $B \geq 0$  and  $dW_1$  and  $dW_2$  are one-dimensional Wiener processes. Let  $a(t)$  be a noise-free trajectory starting at  $a_0$  and  $b(t)$  a noisy trajectory starting at  $b_0$ . If  $\exists b_{max} \geq 0, \forall t \geq 0, 0 \leq E[b(t)] \leq b_{max}$  and  $\exists u_{max} \geq 0, \forall t \geq 0, 0 \leq E[u(t)] \leq u_{max}$ , and  $b_0$  is a deterministic initial condition such that  $b_0 = a_0$ , then  $\forall t \geq 0$ ,

$$E[|a(t) - b(t)|^2] \leq \frac{Ab_{max} + Bu_{max}}{2A}.$$

*Proof.* See Appendix A-2.  $\square$

**Proposition 1.** For a scalar system described by the equation

$$\dot{z} = -Az(t) + Bu(t) + \sqrt{Az(t) + Bu(t)}\Gamma, \quad (19)$$

given that  $E[z(0)] \geq 0$ , if  $\exists u_{max} \geq 0, \forall t \geq 0, 0 \leq E[u(t)] \leq u_{max}$ , then  $\forall t \geq 0$ ,

$$0 \leq E[z(t)] \leq \frac{Bu_{max}}{A} + E[z(0)].$$

*Proof.* See Appendix A-3.  $\square$

### B. Retroactivity Error

As system (6) - (7) is linear, the error due to retroactivity can be found using the same approach as in Section III leading to, for an input of the form  $X = k_1 + k_2 \sin(\omega t)$ ,

$$\frac{|\Delta G_R(j\omega)|}{G_e} = \frac{p_t \omega \delta_1 \delta_2 |k_2|}{X_e \sqrt{(\omega^2 + \delta_2^2)(\omega^2 + \delta_1^2)(\omega^2(p_t + k_{d2})^2 + k_{d2}^2 \delta_1^2)}}, \quad (20)$$

which increases with increasing  $p_t$ .

### C. Noise error

To quantify the error in  $G$  caused by noise inputs we first consider System 3 with the noise input  $\Gamma_Y$ , which causes the error  $\Delta Y_S = Y - Y_R$ , in the upstream system, as introduced in Section III. This error propagates to the downstream system causing an error in the magnitude of the downstream output which we call  $\Delta G_{IS} = G_S - G_R$ . Considering System 2, with the dynamics given in (6) - (7)

and System 3, with the dynamics given in (8) - (9), we obtain the dynamics for  $\Delta G_{IS}$  as

$$\Delta \dot{G}_{IS} = \beta_2 p_t \Delta Y_S / k_{d2} - \delta_2 \Delta G_{IS}. \quad (21)$$

To quantify the error in  $G$  due to  $\Gamma_G$  we determine an upper bound on  $E[|\Delta G_{IS}|^2]$ . For this, we first find an upper bound on  $E[|\Delta Y_S|^2]$  and then use the linearity of (21) to give an upper bound on  $E[|\Delta G_{IS}|^2]$ .

We determine an upper bound on  $E[|\Delta Y_S|^2]$  by applying Corollary 1 with  $a = Y_R$  and  $b = Y$  in systems (6) and (2), respectively. Since  $X(t)$  is the input, we ensure that  $0 \leq X \leq X_{max}, \forall t$ . Next, we verify that  $E[Y] \geq 0$  and that it is upper bounded. Take  $E[Y(0)] > 0$  and apply Proposition 1 to equation (2). It follows that  $E[Y] \geq 0$  and  $E[Y]$  can be upper bounded by the positive constant  $E[Y]_{max}$  such that

$$E[Y]_{max} = \frac{\beta_1 p_{t0} X_{max}}{\delta_1 k_{d1}} + E[Y(0)]. \quad (22)$$

Using that  $\Gamma_Y = dW_Y/dt$  [25] where  $W_Y$ , is a standard Wiener process, and that  $p_t \leq \bar{p}_t < \infty$ , we apply Corollary 1 to systems (6) and (2) to obtain

$$E[|\Delta Y_S|^2] \leq \frac{\left(\frac{k_{d2}}{p_t + k_{d2}}\right)^2 \left[\frac{\beta_1 p_{t0} X_{max}}{k_{d1}} + \delta_1 E[Y]_{max}\right]}{2 \left(\frac{k_{d2}}{p_t + k_{d2}}\right) \delta_1}. \quad (23)$$

Substituting (22) in (23) and simplifying further we have

$$E[|\Delta Y_S|^2] \leq \frac{\left(\frac{k_{d2}}{p_t + k_{d2}}\right) \left[\frac{2\beta_1 p_{t0} X_{max}}{k_{d1}} + \delta_1 E[Y(0)]\right]}{2\delta_1}. \quad (24)$$

To determine an upper bound for  $E[|\Delta G_{IS}|^2]$  we use the linearity of system (21), and denoting by  $R_{yy}(\tau)$ , the auto-correlation of signal  $\Delta Y_S$ , which can be upper bounded by  $R_{yy}(0) = E[|\Delta Y_S|^2]$ , to give

$$E[|\Delta G_{IS}|^2] \leq E[|\Delta Y_S|^2] \left(\frac{\beta_2 p_t}{\delta_2 k_{d2}}\right)^2.$$

Using the upper bound for  $E[|\Delta Y_S|^2]$  in (24), we obtain

$$E[|\Delta G_{IS}|^2] \leq \left(\frac{\beta_2 p_t}{\delta_2 k_{d2}}\right)^2 \frac{\left(\frac{k_{d2}}{p_t + k_{d2}}\right) \left[\frac{2\beta_1 p_{t0} X_{max}}{k_{d1}} + \delta_1 E[Y(0)]\right]}{2\delta_1}.$$

Next, to determine the error in  $G$  due to the perturbation  $\Gamma_G$ , we introduce the error  $\Delta G_S = G - G_S$  where  $G_S$  and  $G$  are outputs of the downstream components in System 3 and System 4, respectively (Fig. 3). To quantify the error due to  $\Gamma_G$ , we find an upper bound for  $E[|\Delta G_S|^2]$  by applying Corollary 1 to equations (9) and (3), with  $a = G_S$  and  $b = G$ . To prove that  $E[G] \geq 0$  and that it can be upper bounded, we apply Proposition 1 to system (3), with  $E[G(0)] > 0$ . This leads to  $0 \leq E[G] \leq E[G]_{max}$ , where

$$E[G]_{max} = \frac{\beta_2 p_t E[Y]_{max}}{\delta_2 k_{d2}} + E[G(0)]. \quad (25)$$

Using the relation that  $\Gamma_G = dW_G/dt$  [25] where  $W_G$  is a standard Wiener process, we can apply Corollary 1 to systems (9) and (3) to obtain

$$E[|\Delta G_S|^2] \leq \frac{\left( \frac{\beta_2 p_t E[Y]_{max}}{k_{d2}} + \delta_2 E[G]_{max} \right)}{2\delta_2}. \quad (26)$$

Substituting (22) and (25) in (26) yields,

$$E[|\Delta G_S|^2] \leq \frac{2\beta_2 p_t \left[ \frac{\beta_1 p_{t0} X_{max}}{k_{d1} \delta_1} + E[Y(0)] \right]}{2\delta_2 k_{d2}} + \frac{E[G(0)]}{2}.$$

Employing the Minkowski inequality we quantify the total error due to noise as

$$\begin{aligned} \frac{\sqrt{E[|\Delta G_P|^2]}}{G_e} &\leq \frac{\sqrt{E[|\Delta G_{IS}|^2]}}{G_e} + \frac{\sqrt{E[|\Delta G_S|^2]}}{G_e}, \\ &\leq \frac{\sqrt{k_{d2} \delta_2 \left[ \frac{\beta_1 p_{t0} X_{max}}{k_{d1} \delta_1} + E[Y(0)] \right]}}{\beta_2 p_t Y_e^2} + \frac{k_{d2} \delta_2 \sqrt{E[G(0)]}}{\sqrt{2} \beta_2 p_t Y_e} \\ &\quad + \frac{\sqrt{\left( \frac{k_{d2}}{p_t + k_{d2}} \right) \left[ \frac{2\beta_1 p_{t0} X_{max}}{k_{d1}} + \delta_1 E[Y(0)] \right]}}{\sqrt{2} \delta_1 Y_e}. \end{aligned} \quad (27)$$

This error decreases with increasing  $p_t$  as illustrated in Fig. 5. Fig. 6 gives a plot of the upper bound of the error due to

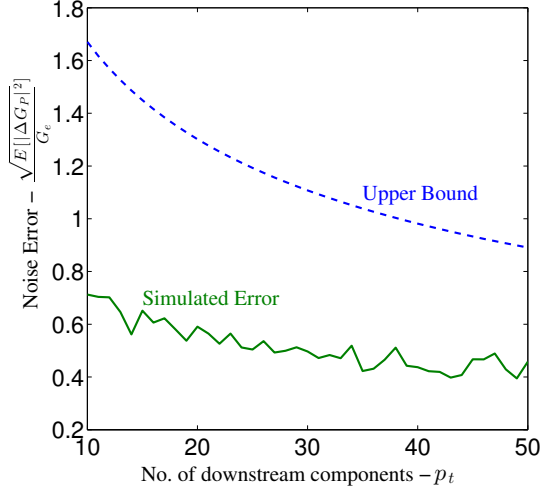


Fig. 5: The upper bound calculate in (27) lies above the simulated error from Systems 2 and System 4. The parameter values are  $X = 0.01(1 + \sin(\omega t))$ nM,  $\beta_1 = 0.001s^{-1}$ ,  $\beta_2 = 0.3s^{-1}$ ,  $\delta_1 = 0.03$ ,  $\delta_2 = 0.01s^{-1}$ ,  $p_{t0} = 100$ nM,  $k_{d1} = 0.1$ nM,  $k_{d2} = 10$ nM,  $\omega = 0.005$  rad/s,  $Y(0) = 1$  and  $G(0) = 1$ . Average of 20 simulations.

noise (27) vs. the error due to retroactivity (20). From this, we can deduce that in order to minimize the upper bound on the error due to noise, we have to increase the error due to retroactivity. Referring to Fig. 1, we can conclude that the precision of the measurement  $G$  is limited by the accuracy of  $Y$ , the quantity to be measured.

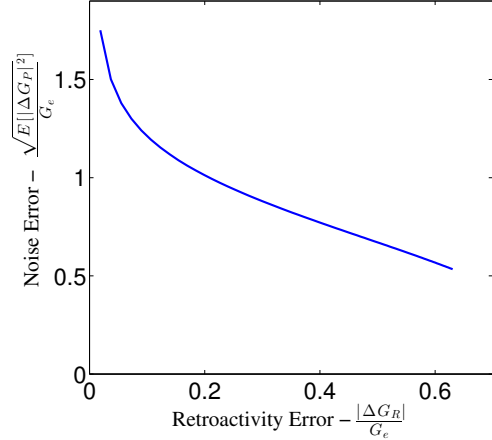


Fig. 6: The trade-off between retroactivity and noise for the nonlinear system. The parameter values are  $X = (1 + \sin(\omega t))$ nM,  $\beta_1 = 0.01s^{-1}$ ,  $\beta_2 = 0.5s^{-1}$ ,  $\delta_1 = 0.01$ ,  $\delta_2 = 0.015s^{-1}$ ,  $p_{t0} = 100$ nM,  $k_{d1} = 50$ nM,  $k_{d2} = 20$ nM,  $Y(0) = 0.001$ nM,  $G(0) = 0.001$ nM and  $\omega = 0.005$  rad/s.

## V. CONCLUSION

In this work, we used tools from linear and nonlinear systems theory to demonstrate the inevitable trade-off between the perturbations caused by retroactivity and noise in connected transcriptional components. We first quantified this trade-off for a linearized system model where we show that reducing the effect of one of the perturbations would lead to an increased error due to the other perturbation. We also demonstrated the trade-off for a nonlinear system model by estimating perturbation due to noise, using and extending results from stochastic contraction theory. The results from this study points towards a fundamental limitation in biomolecular networks that has to be addressed when designing biomolecular circuits.

Similar trade-offs have been identified in measurement of physical systems where the accuracy of the measurement is limited by the perturbation caused by the measurement device [26]. The results from our analysis suggest that natural systems may be subject to similar design trade-offs as engineering systems. They further suggest that biological networks may have evolved optimal design techniques to handle these trade-offs, which may point towards new ways to interpret the organization of natural systems.

## APPENDIX

**A-1:** Following the proof of Lemma 2 in [20], where  $x = (a(t), b(t))^T$  with the Lyapunov-like function  $V(x, t) = (a - b)^T M(t)(a - b)$  and  $L$  denoting the differential generator of the Itô process  $x(t)$  [27], one can prove

$$\forall x, t \quad LV(x, t) \leq -2\lambda V(x, t) + h(x, t) \quad (28)$$

where  $h(x, t) = tr(\sigma(a, t)^T M(t) \sigma(a, t)) + tr(\sigma(b, t)^T M(t) \sigma(b, t))$  and  $LV = \frac{\partial V}{\partial t} + \frac{\partial V}{\partial x} \hat{f}(x, t) + \frac{1}{2} tr(\hat{\sigma}(x, t)^T \frac{\partial^2 V}{\partial x^2} \hat{\sigma}(x, t))$ .

Then, using  $h(x, t)$  in place of  $C$  in equations (II.10) - (II.11) in [20], we obtain

$$\begin{aligned} E_{x_0}[V(x(t), t)] - E_{x_0}[V(x(u), u)] \\ \leq \int_u^t (-2\lambda E_{x_0}[V(x)] + E_{x_0}[h(x, s)])ds. \end{aligned}$$

From (H2), we have  $E_{x_0}[h(x, t)] \leq 2C$  which results in

$$\begin{aligned} E_{x_0}[V(x(t), t)] - E_{x_0}[V(x(u), u)] \\ \leq \int_u^t (-2\lambda E_{x_0}[V(x)] + 2C)ds. \quad (29) \end{aligned}$$

Then, proceeding as in [20], we have

$$\begin{aligned} E(\|a(t) - b(t)\|^2) \\ \leq \frac{1}{\beta} \left( \frac{C}{\lambda} + E((\xi_1 - \xi_2)^T M(0)(\xi_1 - \xi_2))e^{-2\lambda t} \right). \end{aligned}$$

**A-2:** Consider the system (18). Following the proof of Theorem 1 with  $h(x, t) = \text{tr}(\sigma(b, t)^T M(t)\sigma(b, t))$ , leads to  $E_{x_0}[h(x, t)] \leq C$  in place of  $E_{x_0}[h(x, t)] \leq 2C$  in inequality (29), from which we can derive the result (Corollary 1 in [20])

$$\begin{aligned} E(\|a(t) - b(t)\|^2) \\ \leq \frac{1}{\beta} \left( \frac{C}{2\lambda} + E((a_0 - b_0)^T M(0)(a_0 - b_0))e^{-2\lambda t} \right). \quad (30) \end{aligned}$$

We apply this result to system (18) with  $f(a, t) = -Aa(t) + Bu(t)$  and  $\sigma(b, t) = \sqrt{Ab(t) + Bu(t)}$ .

(H1) can be verified by finding the contraction rate of  $f(a, t) = -Aa(t) + Bu(t)$ . We have  $\lambda_{max} \left( \frac{\partial f(a, t)}{\partial a} \right) \leq -\lambda$  and therefore the contraction rate is given by  $\lambda = A$ . To verify (H2), with  $\sigma(b, t) = \sqrt{Ab(t) + Bu(t)}$ , take  $M = I$  so that we have

$$\begin{aligned} E[\text{tr}(\sigma(b, t)^T M\sigma(b, t))] &= E[Ab(t) + Bu(t)], \\ &= AE[b(t)] + BE[u(t)]. \end{aligned}$$

Given that  $0 \leq E[b(t)] \leq b_{max}$  and  $0 \leq E[u(t)] \leq u_{max}$ , we obtain

$$E[\text{tr}(\sigma(b, t)^T M\sigma(b, t))] \leq Ab_{max} + Bu_{max}.$$

Then, applying the result in (30), we find that  $\forall t \geq 0$

$$E[\|a(t) - b(t)\|^2] \leq \frac{Ab_{max} + Bu_{max}}{2A} + E[\|a_0 - b_0\|^2]e^{-2At}.$$

When the initial condition of  $b(t)$  is deterministic and is equal to  $a_0$ , the mean square error is given by

$$E[\|a(t) - b(t)\|^2] \leq \frac{Ab_{max} + Bu_{max}}{2A}.$$

**A-3:** Using the relation  $\Gamma = dW/dt$  [25] where  $W$  is a standard Wiener process, we can write (19) as an Itô differential equation, for which, we get the solution [28]

$$z(t) = z(0) + \int_0^t (-Az(s) + Bu(s))ds$$

$$+ \int_0^t \sqrt{Az(s) + Bu(s)}dW(s) \quad (31)$$

Taking the expected value of both sides in (31) and using that  $E[\int_0^t \sqrt{Az(s) + Bu(s)}dW(s)] = 0$  [28], we have

$$E[z(t)] = E[z(0)] + E \left[ \int_0^t (-Az(s) + Bu(s))ds \right].$$

Taking the derivative with respect to  $t$  and using linearity of expected values, we obtain

$$\frac{dE[z(t)]}{dt} = -AE[z(t)] + BE[u(t)]. \quad (32)$$

Given that  $A > 0$  and  $B \geq 0$ , from (32) we observe that if  $E[u(t)] \geq 0$  and  $E[z(0)] \geq 0 \quad \forall t$ .

Using  $0 \leq E[u(t)] \leq u_{max}$  in (32), we obtain the differential inequality

$$\frac{dE[z(t)]}{dt} \leq -AE[z(t)] + Bu_{max}, \quad (33)$$

which leads to (Theorem 9.5 in [29])

$$E[z(t)] \leq \frac{Bu_{max}}{A} + E[z(0)], \quad \forall t \geq 0.$$

## REFERENCES

- [1] U. Alon. Biological networks : Tinkerer as an engineer. *Science*, 301:1866–1867, 2003.
- [2] L.H Hartwell, J.J. Hopfield, S. Leibler, and A.W.Murray. From molecular to modular cell biology. *Nature*, 402:C47–52, 1999.
- [3] R. Milo, S. Shen-Orr, S. Itzkovitz, N.Kashtan, D.Chklovskii, and U.Alon. Network motifs : Simple building blocks of complex networks. *Science*, 298:824–827, 2002.
- [4] J. Saez-Rodriguez, A. Kremling, and E.D. Gilles. Dissecting the puzzle of life: modularization of signal transduction networks. *Computers and Chemical Engineering*, 29(3):619–629, 2005.
- [5] P. E. M. Purnick and R. Weiss. The second wave of synthetic biology: from modules to systems. *Nature Reviews Molecular Cell Biology*, 2009.
- [6] D. Del Vecchio, A. J. Ninfa, and E. D. Sontag. Modular cell biology: retroactivity and insulation. *Mol Syst Biol*, 2008.
- [7] K. Kim and H. Sauro. Fan-out in gene regulatory networks. *Journal of Biological Engineering*, 4(1):16, 2010.
- [8] S. Jayanthi, K. S. Nilgiriwala, and D. Del Vecchio. Retroactivity controls the temporal dynamics of gene transcription. In *ACS Synthetic Biology*, 2013.
- [9] P. Jiang, A. C. Ventura, E. D. Sontag, S. D. Merajver, A. J. Ninfa, and D. Del Vecchio. Load-induced modulation of signal transduction networks. *Science Signaling*, 2011.
- [10] N. Rosenfeld, J. W. Young, U. Alon, P. S. Swain, and M. B. Elowitz. Gene regulation at the single-cell level. *Science*, 307(5717):1962–1965, 2005.
- [11] M.B. Elowitz, A.J.Levine, E.D.Siggia, and P.S.Swain. Stochastic gene expression in a single cell. *Science*, 297, 2002.
- [12] P. S. Swain, M. B. Elowitz, and E.D. Siggia. Intrinsic and extrinsic contributions to stochasticity in gene expression. In *Proc. Natl Acad. Sci. USA* 99, 2002.
- [13] J. Paulsson. Summing up the noise in gene networks. *Nature*, 427, 2004.
- [14] J. M. Raser and E. K. O’Shea. Noise in gene expression: Origins, consequences, and control. *Science*, 309(5743):2010–2013, 2005.
- [15] E. Schrödinger. *What is Life?* Cambridge University Press, 1944.
- [16] J. Elf and M. Ehrenberg. Fast evaluation of fluctuations in biochemical networks with the linear noise approximation. *Genome Research*, 2003.
- [17] Y. Pilpel R. Kafri, M. Springer. Genetic redundancy: New tricks for old genes. *Cell*, 136(3):389–392, 2009.

- [18] S. Jayanthi and D. Del Vecchio. On the compromise between retroactivity attenuation and noise amplification in gene regulatory networks. In *Proc. of IEEE Conference on Decision and Control*, 2009.
- [19] K. Kim and H. Sauro. Measuring retroactivity from noise in gene regulatory networks. *Biophysical Journal*, 100(5):1167 – 1177, 2011.
- [20] Q. Pham, N. Tabareau, and J. Slotine. A contraction theory approach to stochastic incremental stability. In *IEEE Transactions on Automatic Control*, 2009.
- [21] H. K. Khalil. *Nonlinear Systems*. Addison-Wesley, 2002.
- [22] Daniel T Gillespie. Stochastic simulation of chemical kinetics. *Annu. Rev. Phys. Chem.*, 58:35–55, 2007.
- [23] A. Papoulis. *Probability, Random Variables, and Stochastic Processes*. McGraw-Hill, Inc, 1991.
- [24] D. Del Vecchio and J. Slotine. A contraction theory approach to singularly perturbed system with applications to retroactivity. In *Proc. of IEEE Conference on Decision and Control*, 2011.
- [25] B. Oksendal. *Stochastic Differential Equations : an introduction with applications*. Springer, 1998.
- [26] H.Sandberg and J. Delvenne. The observer effect in estimation with physical communication constraints. In *Proc. of the 18th IFAC World Congress*, 2011.
- [27] H. Kushner. *Stochastic Stability and Control*. Academic Press, 1967.
- [28] E. Allen. *Modeling with Itô stochastic differential equations*. Springer, 2007.
- [29] J. Szarski. *Differential Inequalities*, page 27. PWN - Polish Scientific Publishers, 1965.